# Non-local Means Kernel Regression based Despeckling of B-mode Ultrasound Images

R Bharath and P Rajalakshmi
Department of Electrical Engineering,
Indian Institute of Technology Hyderebad,
email:{ee13p0007, raji }@iith.ac.in

***Abstract*— Medical ultrasound scanning is a widely used diagnostic imaging modality in health-care. Speckle is inherent noise present in ultrasound images reducing the diagnostic accuracy of ultrasound scanning. Speckle noise contributes to high variance between pixels and delineates boundaries of the organs. Effective despeckling involves reducing the variance between pixels corresponding to homogeneous region and to preserve anatomical details simultaneously. Non-Local Means filters are highly successful and produced state of the art results in despeckling ultrasound images. In this paper, we show the effectiveness of Non-Local Means filter with polynomial regression kernel in despeckling ultrasound images. The proposed algorithm is evaluated on software simulated and real time ultrasound images and proved very effective in both despeckling and edge preservation.**

***Index Terms*— kernel regression, multiplicative noise, non-local Means, speckle filtering, ultrasound scanning.**

## I. INTRODUCTION

Ultrasound images are affected with a multiplicative noise termed as speckle. The speckle noise appears as *dense granules* and *small worm* like structures in the image. The speckle noise increases the variance between adjacent pixels, delineates the contour, masks the fine information about tissues, thus reducing the diagnostic accuracy of the ultrasound scanning machine. Ultrasound image restoration involves reducing the variance in homogeneous region and preserving the edges simultaneously. Signal dependent nature of speckle should be taken care while designing a filter for speckle suppression to preserve anatomical details present in an image.

In this paper, we used local polynomial regression kernel as an extension to Non-local Means (NLM) approach. The proposed approach is strongly motivated from the findings of [1]. NLM approach [2] gave state of the art results in removing Gaussian noise in natural images. NLM approach is extended in [3] with Bayesian inference to effectively suppress the speckle noise in ultrasound images. In [4] , modified NLM approach is employed to despeckle the image, in this method first maximum likelihood estimation is employed to estimate the noise free pixel and then NLM is applied to restore the pixel.

The significance of regression kernels in image restoration is discussed in [5]. In [6], the NLM approach is generalized via polynomial regression kernel and shown that higher degrees of polynomial can get better results in denoising the image. In this paper, we show the effectiveness of local polynomial regression kernel with NLM framework in despeckling the ultrasound image.

Despeckling filters proposed in the literature depends on local statistics of the pixel, where the local statistics of the pixel corresponds to mean, variance etc., computed around the neighborhood of a pixel. The common factor seen from most of the despeckling filters is smoothing, and is differed by the way how it smooths. The filters proposed in [7], [8], [9] are based on the same principle, these filters reduce the variance by smoothing the pixels in homogeneous region and preserves the edges by unaltering the pixels near the edges. Filters proposed in [10], [11], [12] are motivated from heat diffusion and gave state of the art results in preserving the edges along with speckle suppression but suffers from over smoothing result in loosing texture information present in the image. Ultrasound despeckling through sparse and overcomplete representations are proposed in [13], [14].

Despeckling of ultrasound image is measured with respect to speckle suppression and edge preservation, so to quantify the performance of the filter, we need more than one metric. In this paper, we used four metrics each specific to speckle suppression, edge preservation and anatomy structure preservation. The computation and significance of each metric is discussed in results section. The performance of the proposed filter is compared with Frost [7], Lee [8], Adaptive Weighted Median Filter (AWMF) [9], SRAD [10] and Optimized Bayesian Non-local Means (OBNLM) [3]. The algorithms are tested on Field II software [15] simulated ultrasound kidney image and real ultrasound liver image. Metrics are computed for software simulated ultrasound kidney image and despeckled images of real ultrasound liver images are presented for visual comparison.

## II. PROPOSED METHOD

In this paper, we assume noise in the final image behaves as additive Gaussian noise, the additiveness comes from the application of log operation, which is used for dynamic range compresion of RF data, and Gaussian assumption for speckle noise is motivated from [16]. The ultrasound image after log compression is modeled in the following way

$$y_i = z(x_i) + \eta_i \tag{1}$$

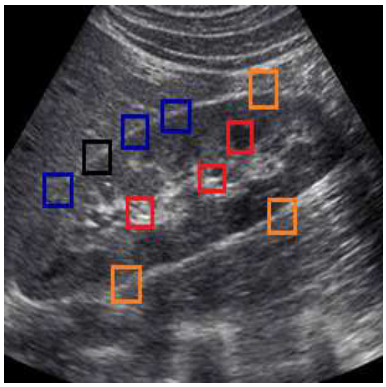

Fig. 1: Graphical representation of similar patches occurring in real ultrasound kidney image.

where $y_i$ represents observed pixel intensity at spatial position $x_i$, $z(.)$ is noise free pixel corrupted with noise $\eta$, $x_i = [x_1 \;\; x_2]_i^T$, $i \in$ cardinality of the image. The objective of despeckling filter is to estimate noise free version of the pixel from $y_i$. Spatially adaptive speckle suppression filters proposed in the literature are based on the local neighborhood of data [7], [8], [9]. NLM takes a different approach to resolve local pixels by comparing with nonlocal patches (pixel of interest is the center of the patch). The NLM make use of similar patches occurring in image and use this similar patches to denoise the image, assuming the noise in image is uncorrelated. Fig. 1 shows the similar patches present in ultrasound image, the similar patterns of black box is represented with blue boxes, dissimilar patches with red boxes and intermediate one with orange boxes.

Computing the similar patches for each pixel in entire image is a computationally expensive procedure. To reduce the computations, the search space for finding the similar patches is restricted to local neighborhood and this is very much justified as the probability of getting similar patches reduces as the patch moves away from the pixel of interest. In [3], computations are further reduced by block wise processing of patches instead of pixel wise processing. NLM uses weighted averaging of pixels, where amount of weight assigned to each pixel depends upon the similarity of the patch with respect to patch corresponding to pixel under consideration. This can be written mathematically as

$$\hat{z}(x_i) \quad = \frac{1}{C_i} \sum_{j \in I} w_{ij} y_j, \quad where \quad C_i \quad = \sum_j w_{ij} \quad (2)$$

$C_i$ is a normalizing constant and the index $j$ runs over the entire search space of the corresponding pixel of interest. $w_{ij}$ is the weight assigned for each pixel based on the similarity between neighborhood of a pixel present in the search space with respect to the pixel of interest. The weights for a particular pixel is computed as

$$w_{ij} = e^{-\frac{||V(x_i) - V(x_j)||_a^2}{h}} \quad (3)$$

where $V(x_i)$ is the vectored version of a patch centered at location $x_i$, $h$ is a global smoothing parameter controlling the amount of smoothing in the denoising process and $a$ is the variance of the Gaussian distribution used to give decaying weights for the pixels located away from the pixel of interest. The weight computation mechanism given in equation (3) assigns high weight to the similar patches and low weight to the dissimilar patches. These weights determine the contribution of central pixels in a patch to estimate the despeckled pixel intensity. The equivalent noise free estimation of pixel is modeled as an optimization problem in the following way.

$$\begin{aligned} \hat{z}(x_i) \quad &= arg \min_{z(x_i)} \sum_{j=1}^{P} (y_j - z(x_i))^2 w_{ij} \\ &= arg \min_{z(x_i)} \parallel Y_i - 1z(x_i) \parallel_{W_i}^2 \end{aligned} \quad (4)$$

here $Y_i$ stands for lexicographically ordered vectored version of $P$ pixels within the search window centered around the pixel value $x_i$. 1 corresponds to column vector with all ones. Equation (4) can be seen as the cost function trying to compute a single constant at each pixel location, which minimizes the error in reconstruction of the patch under consideration.

The weights are computed likewise within the search window resulting $W = diag[w_{i1}...w_{ij}...w_{iP}]$. The intuition about weights is to penalize the pixel value which has more dissimilarity in restoring the pixel. This method does not make the approach NLM due to limiting the search space to local neighborhood. The better performance is obtained for larger neighborhood. In a global sense, the NLM assumes that the image is modeled as local constancy throughout the image. Assumption of local constancy does not hold well in the presence of finer structures and as a result we can see lack of texture in the despeckled image.

The assumption of local constancy is generalized by assuming the image is locally sufficiently smooth, Taylor expansion for the pixel of interest can be written as

$$\begin{aligned} z(x_j) &= z(x_i) + \{\nabla z(x_i)\}^T (x_j - x_i) + \\ &\quad \frac{1}{2}(x_j - x_i)^T \{H(z(x_i))\}(x_j - x_i) + .... \end{aligned}$$

$$\begin{aligned} z(x_j) &= z(x_i) + \{\nabla z(x_i)\}^T (x_j - x_i) + \\ &\quad \frac{1}{2} vech^T \{H(z(x_i))\} vech\{(x_j - x_i)(x_j - x_i)^T\} + .... \end{aligned} \quad (5)$$

where $\nabla$ is a $2 \times 1$ gradient operator, $H$ is a $2 \times 2$ Hessian operator, and vech(.) is a half vectorization operation which lexicographically order a matrix into vector form. The vech(.) of a symmetric matrix is defined as

$$vech\left( \begin{bmatrix} l & m & n \\ m & o & p \\ n & p & r \end{bmatrix} \right) = [l \quad m \quad n \quad o \quad p \quad r]^T \quad (6)$$

Considering the symmetry of Hessian matrix, equation (5) is rewritten as

$$\begin{aligned} z(x_j) &= \beta_{\{0\}i} + \beta_{\{1\}i}^T (x_j - x_i) + \\ &\quad \beta_{\{2\}i}^T vech\{(x_j - x_i)(x_j - x_i)^T\} + .... \end{aligned} \quad (7)$$

where $\beta_1$ and $\beta_2$ are defined as

$$\beta_1 = \quad \nabla z(x) = \left[\frac{\partial z(x)}{\partial x_1}, \quad \frac{\partial z(x)}{\partial x_2}\right]^T \tag{8}$$

$$\beta_2 = \quad \frac{1}{2}\left[\frac{\partial^2 z(x)}{\partial x_1^2}, \quad \frac{\partial^2 z(x)}{\partial x_1 \partial x_2}, \quad \frac{\partial^2 z(x)}{\partial x_2^2}\right]^T \tag{9}$$

(7) can be written to all the pixels in the search window centered at any given pixel. The fidelity of the expression diminishes as we move away from the center of the pixel. The expansion of the expression is restricted to some order, say *K* and the pixel value which best fits (7) is the despeckled pixel intensity. By minimizing the cost function with respect to unknown $\beta_i$ parameters, we can compute despeckled pixel intensity. $\beta_i$ parameters are computed by solving the objective function

$$\begin{aligned}\hat{\beta}_i = arg\min_{\beta_i} \sum_{j=1}^{K} (y_j - \beta_{\{0\}i}^T - \beta_{\{1\}i}^T (x_j - x_i) - \\ \beta_{\{2\}i}^T vech\{(x_j - x_i)(x_j - x_i)^T\} + ...)^2\end{aligned} \tag{10}$$

Above equation can be written in matrix form as

$$\hat{\beta}_i = arg\min_{\beta_i} \sum_{j=1}^{K} \parallel Y - \phi\beta_i \parallel_{W_i}^2 \tag{11}$$

$$\hat{\beta}_i = arg\min_{\beta_i} \sum_{j=1}^{K} (y - \phi\beta_i)^T W (y - \phi\beta_i)$$

where $Y = [y_1, y_2, y_3 ... y_K]^T$, $\beta_i = [\beta_0, \beta_1, \beta_2, ... \beta_N]$,

$$\phi = \begin{bmatrix} 1 & (x_1 - x_i)^T & vech^T\{(x_1 - x_i)(x_1 - x_i)^T\} & .. \\ 1 & (x_2 - x_i)^T & vech^T\{(x_2 - x_i)(x_2 - x_i)^T\} & .. \\ . & . & . & .. \\ . & . & . & .. \\ 1 & (x_K - x_i)^T & vech^T\{(x_K - x_i)(x_K - x_i)^T\} & .. \end{bmatrix} \tag{12}$$

$$\beta_i = \left[\beta_{\{0\}i}, \beta_{\{1\}i}, \beta_{\{2\}i} ...\right]^T \tag{13}$$

The matrix $\phi$ is formed from polynomial basis vectors and $\beta_i$ is a vector. After computing the elements in $\beta_i$, the denoised pixel intensity value is replaced with $\beta_{\{0\}i}$ element under local polynomial data model assumption. Mathematically the despeckled pixel intensity is given by

$$\hat{z}(x_i) = c^T \phi \hat{\beta}_i = \hat{\beta}_{\{0\}i} \tag{14}$$

where $c^T = [0 \ 0 \ . \ 1 \ . \ 0 \ 0]$, one in the array corresponds to the central pixel in the patch. Equation (11) has a closed form solution and it is given by

$$\hat{\beta}_i = (\phi^T W_i \phi)^{-1} \phi^T W_i y_i = E_i y_i \tag{15}$$

The matrix $E_i$ is the equivalent kernel used to perform weighted averaging process. From equation (14), the despeckled intensity value at position $x_i$ is retained as $\hat{z}(x_i) = \hat{\beta}_{\{0\}i}$. The generalization of NLM with zero-th order polynomial regression kernel is obtained by taking only first column of the $\phi$ matrix in equation (12)

$$\hat{\beta}_i = (1^T W_i 1)^{-1} 1^T W_i y_i = \frac{1^T W_i y_i}{1^T W_i y_i 1} = \frac{\sum_{j=1}^{P} w_{ij} y_j}{\sum_{j=1}^{P} w_{ij}} \tag{16}$$

The higher orders of polynomial regression with NLM is dependent on number of terms we retain in Taylor series expansion. In this paper, the results are reported for first and second order NLM polynomial regression kernel. The first and second order NLM polynomial regression is obtained by taking first two and three columns of $\phi$ matrix respectively.

## III. Experimental Results

The experiments are conducted on Field II simulated left kidney image. The kidney phantom image shown in Fig.2a is downloaded from [17]. The speckles in ultrasound image is generated by placing one lakh scatters randomly throughout the phantom image. The scatter amplitude of the tissue is modeled with Gaussian distribution with variance depending on the cross section of the tissue. The phantom is scanned with a 7 MHz, 128 element phased array transducer with half of the wavelength spacing between elements and Hanning apodization is used to suppress the side lobes. A single transmit focus 60 mm from the transducer is used, and focusing during reception is at 5 to 150 mm in 1 mm increments. The image consists of 128 scan lines with 0.7 degrees between lines. The kidney phantom and its corresponding ultrasound image is shown in Fig.2.

The performance of algorithms are evaluated using the following metrics.

### A. Conventional speckle SNR ($\alpha$)

Conventional speckle SNR $\alpha$ is used as a measure to quantify amount of speckle noise present in an image. $\alpha$ is defined as ratio of mean to the standard deviation of pixels present in homogeneous region of an image [18]. The higher values of $\alpha$ implies the goodness of the filter in suppressing the speckle noise.

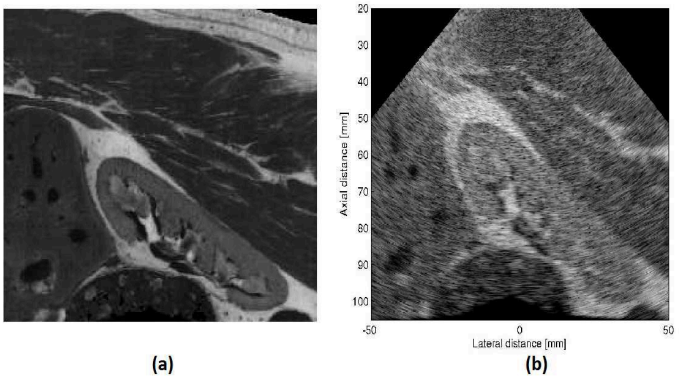


Fig. 2: (a) Kidney phantom image. (b) Simulated ultrasound image of (a)

### B. Despeckling index (J)

The Despeckling index $J$ measures how well a filter reduce variances in homogeneous region while keeping other classes well separated [19]. $J$ is based on modified Fisher discriminant contrast metric and it is computed as

$$J(alg) = \frac{\sum\limits_{m \neq n} (\mu c_m - \mu c_n)^2}{\sum\limits_{m=1}^{3} \sigma_m^2} \tag{17}$$

where

$$\mu c_m = \frac{1}{|c_m|} \sum_{(i,j) \in c_k} I_{alg}(i,j)$$

$$\sigma^2 c_m = \frac{1}{|c_m|} \sum_{(i,j) \in c_k} (I_{alg}(i,j) - \mu c_m)^2$$

$|c_m|$ represents number of pixels in cluster $m$, $I_{alg}$ represents despeckled image and $m$ represents number of clusters used in an image. In this paper, we used three clusters to compute $J$. The quantity $J$ is sensitive to resolution, to avoid this, equation (17) is normalized with $J$ of speckle image ($J_{spk}$).

$$\tilde{J}_{alg} = \frac{J_{alg}}{J_{spk}}$$

Higher the value of $\tilde{J}_{alg}$, better is the performance of the filter in despeckling.

### C. Figure of Merit (FOM)

In this paper, we choose Pratt Figure of Merit $FOM$ [20] to measure the performance of despeckling filter in preserving the edges. $FOM$ is defined as

$$FOM = \frac{1}{max\{N_{tem}, N_{alg}\}} \sum_{i=1}^{N_{tem}} \frac{1}{1 + d_i^2 \gamma} \tag{18}$$

$N_{tem}, N_{alg}$ are the edge pixels of template and despeckled image respectively, $d_i$ is the Euclidean distance between the $i^{th}$ edge pixel in template image to the nearest edge pixel in despeckled image, $\gamma$ is a constant typically set to $1/9$. $FOM$ lies in between 0 and 1, and for ideal edge detector $FOM$ equals to 1. The binary edge map of the images are obtained using canny edge operator by setting standard deviation of Gaussian kernel equal to 1.414.

### D. Mean Structural Similarity Index (MSSIM)

MSSIM of a despeckled image gives how well a despeckled image preserves the information like contrast, luminance and structure with respect to original image [21]. Structural Similarity Index (SSIM) is computed for every pixel over local neighborhood and it is given by

$$SSIM(i,j)_{I,J} = L_{I,J}(i,j) C_{I,J}(i,j) S_{I,J}(i,j) \tag{19}$$

here $L, C, S$ represents the luminance, contrast, structural similarity between $i$ and $j$ pixels corresponds to image $I$

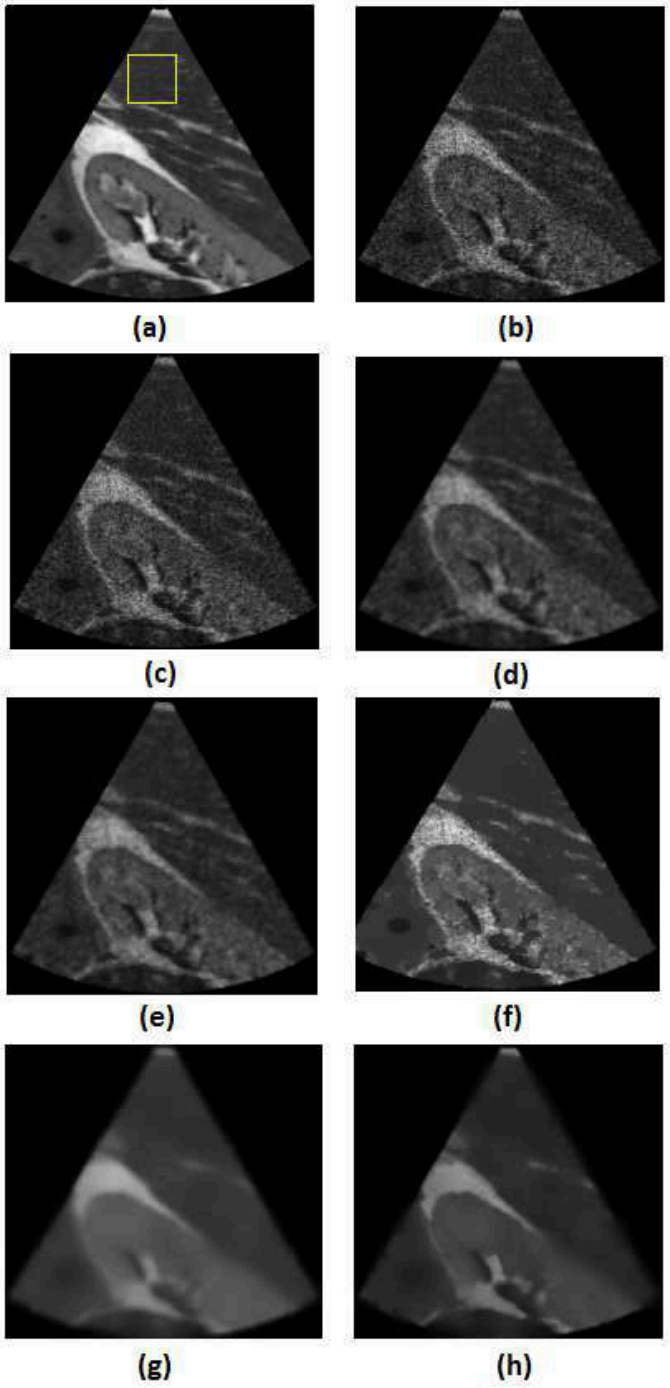


Fig. 3: (a). Kidney phantom. (b) simulated ultrasound kidney image. Visual comparison of various despeckling filters on (b): (c) Lee. (d) Frost. (e) AWMF. (f) SRAD. (g) OBNLM. (h) Proposed method.

and $J$ respectively. MSSIM is defined as the mean of SSIM and is given by

$$MSSIM = \frac{1}{MN} \sum_{i=1}^{N} \sum_{j=1}^{M} SSIM_{I,J}(i,j) \tag{20}$$

$MN$ represents the cardinality of the image. MSSIM lies in the range between -1 and 1, and for the ideal edge preserved

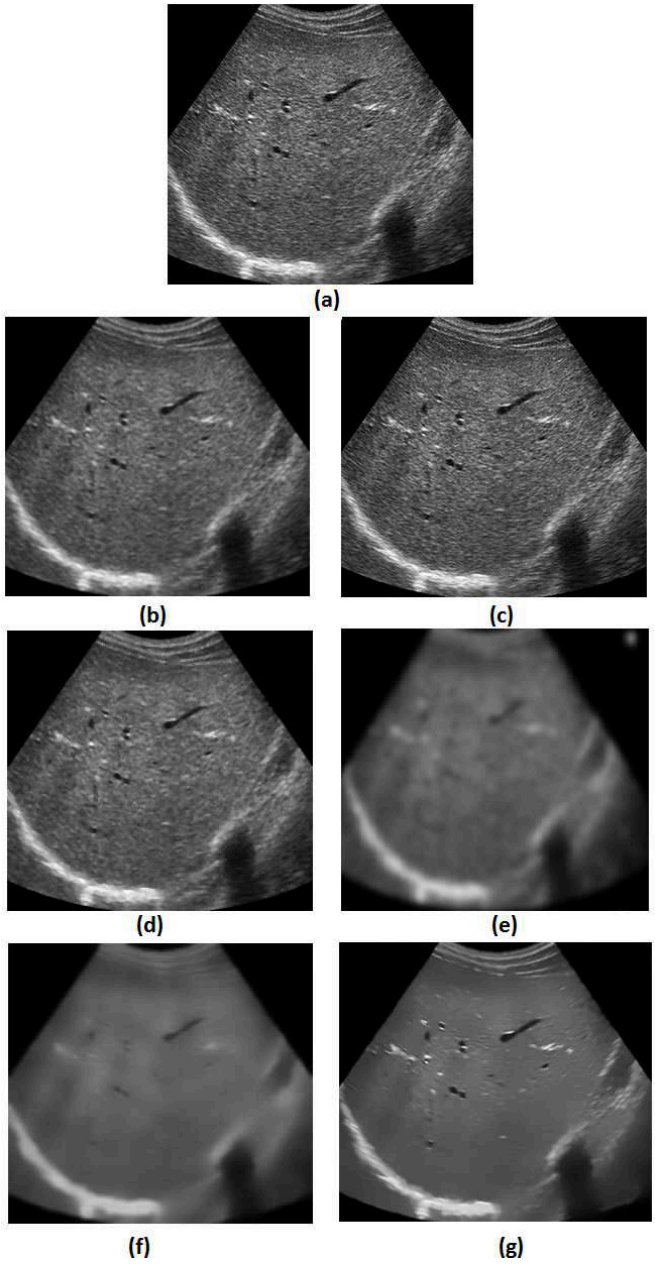


Fig. 4: (a). Real Liver ultrasound image. Visual comparison of various despeckling filters on (a): (b) Frost. (c) Lee. (d) AWMF. (e) SRAD. (f) OBNLM. (g) Proposed method with Order 2.

image MSSIM is going to be 1.

The result of various despeckling filters applied on kidney phantom image is shown in Fig. 3. The optimal filter parameters for the filter with respect to $\alpha$ metric is shown in Table.1. The metric values for various filters for simulated kidney phantom image is shown in Table. II. The proposed method give high values with $\alpha = 18.7251$ and $J = 1.0627$ for zero-$th$ polynomial order, $FOM = 0.5679$ is obtained for first order, and $SSIM = 0.7886$ is obtained for second order polynomial. Proposed method resulted with better performance with respect to $\alpha, J, FOM$ compared to other filters and AWMF performed well above all despeckling filters with respect to $MSSIM$ with 0.8013

The results of various despeckling filters on live ultrasound image is shown in Fig.4. Perceptually, we can see the effectiveness of proposed algorithm in improving the visual quality of the liver image compared to other filters.

TABLE I: Optimal parameters used for the filters for Fig. 3 with respect to metric evaluation. $W$: window size, $I_t$: Number of iterations, $\sigma$: Smoothing Parameter, $N$: Polynomial order, $\Delta$: Search window.

| Filter | Optimized parameters |
|---|---|
| Lee | $W$=5×5 |
| Frost | $W$=5×5 |
| AWMF | $W$=7×7 |
| SRAD | $I_t$=1500, $\sigma$=0.5 |
| OBNLM | $\sigma$=15, 20; $W$=5×5, $\Delta$=15 × 15. |
| Proposed Method | $\sigma$=15, 20; $N$=0,1,2 ; $W$=5×5, $\Delta$=15 × 15. |

TABLE II: Comparison of various despeckling filters for kidney phantom image shown in Fig .3. $\alpha$ is computed for the window shown in Fig .3a.

| Filter | $\alpha$ | J | FOM | MSSIM |
|---|---|---|---|---|
| Noisy | 4.9071 | - | 0.4549 | 0.7115 |
| Lee | 4.9071 | 0.9985 | 0.4549 | 0.7126 |
| Frost | 9.1108 | 0.9982 | 0.4560 | **0.8013** |
| AWMF | 8.8955 | 0.9406 | 0.4246 | 0.7921 |
| SRAD | 6.5032 | 0.8044 | 0.4168 | 0.7175 |
| OBNLM | 14.7969 | 0.7392 | 0.3883 | 0.7320 |
| Proposed Metod | **18.7251** | **1.0627** | **0.5679** | 0.7886 |

The visual comparison of proposed method with respect to different polynomial orders on liver ultrasound images is shown in Fig.5. The residual image is computed by subtracting the filtered image with original image. The shape patterns in residual image infers that along with speckles the filter removes the useful information present in the image. Less the patterns in the residual image, better is the performance of the filter in preserving information. From Fig.5, we can infer that as the order of the polynomial increases, patterns in residual image also reduces resulting in better preservation of information in an ultrasound image.

The live ultrasound image is acquired through Toshiba Capasee SSA-220A ultrasound scanner. From the despeckled images of liver, we notice that SRAD and OBNLM filter oversmoothes an image resulting in blurring. Frost, Lee and AWMF filters preserves the texture in the image, but fail to effectively suppress the speckle noise. The proposed algorithm effectively suppressed the speckle noise without deblurring the image, preserving the edges and contrast of the image. Perceptually the despeckled image of the proposed algorithm is also of high quality compared to other despeckling filters. The despeckling algorithms are realized using MATLAB software on a PC powered with Intel core i5 processor, 8GB RAM running with 2.6 GHz clock speed. The algorithm took 37.18, 50.92, 52.52 seconds for

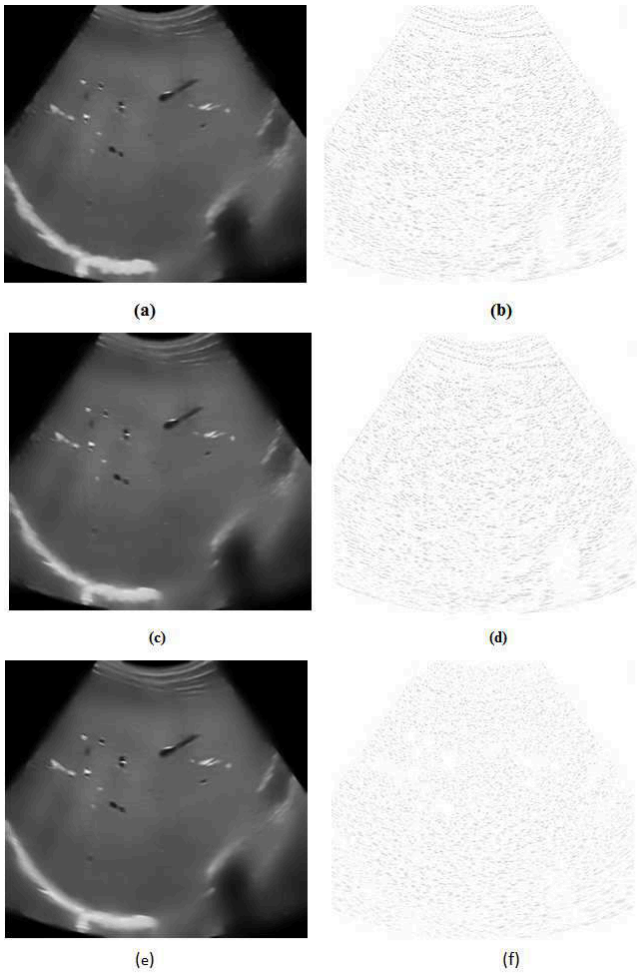


Fig. 5: (a) Order 0 filtered image. (b) Order 0 residual image. (c) Order 1 filtered image. (d) Order 1 residual image. (e) Order 2 filtered image. (f) Order 2 residual image.

executing the proposed method of zero-th, first and second order respectively for the kidney phantom image which is of size $179 \times 187$.

## IV. Conclusion

In this paper, we extended the Non-Local Means approach with polynomial regression kernel for despeckling the ultrasound images. The proposed algorithm on kidney phantom simulated image performed better with respect to conventional signal to noise ratio ($\alpha$), Despeckling index ($J$) and Pratt Figure of Merit ($FOM$). The optimal results of the proposed algorithm with respect to $\alpha$ and $J$ is obtained for zero-th order polynomial, $FOM$ is obtained for first order polynomial, $MSSIM$ is obtained for second order polynomial. It is noted that as the polynomial order increases, the filter better preserves the texture. The proposed algorithm effectively despeckle the image without deblurring and also preserve the edges in the image. No same order polynomial is able to produce the best results with respect to all the metrics. Finding an optimal polynomial order to get good results with respect to all metrics will be useful in proposed approach which is the future scope of work.

## References

[1] Arias-Castro, Ery, Joseph Salmon, and Rebecca Willett. "Oracle inequalities and minimax rates for nonlocal means and related adaptive kernel-based methods." SIAM Journal on Imaging Sciences 5, no. 3 (2012): 944-992.

[2] Buades, Antoni, Bartomeu Coll, and Jean-Michel Morel. "A review of image denoising algorithms, with a new one." Multiscale Modeling & Simulation 4, no. 2 (2005): 490-530.

[3] Coupe, Pierrick, Pierre Hellier, Charles Kervrann, and Christian Barillot. "Nonlocal means-based speckle filtering for ultrasound images." Image Processing, IEEE Transactions on 18, no. 10 (2009): 2221-2229.

[4] Guo, Y., Y. Wang, and T. Hou. "Speckle filtering of ultrasonic images using a modified non local-based algorithm." Biomedical Signal Processing and Control, Elsevier, 6, no. 2 (2011): 129-138.

[5] Takeda, Hiroyuki, Sina Farsiu, and Peyman Milanfar. "Kernel regression for image processing and reconstruction." Image Processing, IEEE Transactions on 16, no. 2 (2007): 349-366.

[6] Chatterjee, Priyam, and Peyman Milanfar. "A generalization of non-local means via kernel regression." In Electronic Imaging 2008, pp. 68140P-68140P. International Society for Optics and Photonics, 2008.

[7] Frost, Victor S., Josephine Abbott Stiles, K. Sam Shanmugan, and Julian C. Holtzman. "A model for radar images and its application to adaptive digital filtering of multiplicative noise." Pattern Analysis and Machine Intelligence, IEEE Transactions on 2 (1982): 157-166.

[8] Lee, Jong-Sen. "Digital image enhancement and noise filtering by use of local statistics." Pattern Analysis and Machine Intelligence, IEEE Transactions on 2 (1980): 165-168.

[9] Loupas, T., W. N. McDicken, and P. L. Allan. "An adaptive weighted median filter for speckle suppression in medical ultrasonic images." Circuits and Systems, IEEE Transactions on 36, no. 1 (1989): 129-135.

[10] Yu, Yongjian, and Scott T. Acton. "Speckle reducing anisotropic diffusion." Image Processing, IEEE Transactions on 11, no. 11 (2002): 1260-1270.

[11] Gupta, Deep, R. S. Anand, and Barjeev Tyagi. "Despeckling of ultrasound medical images using nonlinear adaptive anisotropic diffusion in nonsubsampled shearlet domain." Biomedical Signal Processing and Control, Elsevier, 14 (2014): 55-65.

[12] Wang, Guodong, Jie Xu, Zhenkuan Pan, and Zhaojing Diao. "Ultrasound image denoising using backward diffusion and framelet regularization." Biomedical Signal Processing and Control, Elsevier, 13 (2014): 212-217.

[13] Deka, Bhabesh, and Prabin Kumar Bora. "Removal of correlated speckle noise using sparse and overcomplete representations." Biomedical Signal Processing and Control, Elsevier, 8, no. 6 (2013): 520-533.

[14] Srinivas, M., R. Bharath, P. Rajalakshmi, and C. Krishna Mohan. "Sparseland model for speckle suppression of B-mode ultrasound images." In Communications (NCC), 2015 Twenty First National Conference on, pp. 1-6. IEEE, 2015.

[15] Jensen, Jrgen Arendt. "Field: A program for simulating ultrasound systems." In $10^{th}$ Nordicbaltic Conference on Biomedical Imaging, vol. 4, supplement 1, part 1: 351–353. 1996.

[16] Odegard, Jan E., Haitao Guo, Markus Lang, C. Sidney Burrus, Raymond O. Wells Jr, Leslie M. Novak, and Margarita Hiett. "Wavelet-based SAR speckle reduction and image compression." In SPIE's 1995 Symposium on OE/Aerospace Sensing and Dual Use Photonics, pp. 259-271. International Society for Optics and Photonics, 1995.

[17] http://field-ii.dk/

[18] Wagner, Robert F., Stephen W. Smith, John M. Sandrik, and Hector Lopez. "Statistics of speckle in ultrasound B-scans." Sonics and Ultrasonics, IEEE Transactions on 30, no. 3 (1983): 156-163.

[19] Tay, Peter C., Scott T. Acton, and John Hossack. "Ultrasound despeckling using an adaptive window stochastic approach." In Image Processing, 2006 IEEE International Conference on, pp. 2549-2552. IEEE, 2006.

[20] W. K. Pratt, Digital Image Processing. New York: Wiley, 1977.

[21] Wang, Zhou, Alan Conrad Bovik, Hamid Rahim Sheikh, and Eero P. Simoncelli. "Image quality assessment: from error visibility to structural similarity." Image Processing, IEEE Transactions on 13, no. 4 (2004): 600-612.